A Stochastic Metric-Topological Neighbor Rule for the Vicsek Model

Rene-Marcel Lehner
Department of Physics, TU Dortmund University

Condensed manuscript of the bachelor thesis “Analyse und Simulation neuronaler Schwarmdynamik” (TU Dortmund University, Kierfeld group, 2023). Prepared in 2026.

Abstract. Collective motion models describe how simple local rules produce coherent swarms. A central modeling choice is how each agent selects its neighbors: metric models use all agents within a fixed radius, topological models use a fixed number of nearest neighbors. Purely topological selection destabilizes the classic Vicsek model and produces fragmented micro-flocks. This thesis introduced a stochastic metric-topological rule: each agent draws k neighbors uniformly at random from all agents within its metric radius, resampled at every time step. The sampled average is an unbiased Monte Carlo estimate of the full Vicsek interaction, with k acting as the sample size. In simulations with up to $N = 2000$ agents, the rule removes the fragmentation of the topological model and reproduces Vicsek behavior under the evaluated observables. The mean squared deviation of the order parameter falls rapidly with k; for $k = 6$ the two models are nearly indistinguishable. A second part of the thesis explored multi-agent reinforcement learning (MARL) as a way to replace hand-written interaction rules with learned ones. An actor-critic pipeline around the C++ simulation was implemented and ran end to end, but training did not produce an interpretable policy. That part is reported as a documented negative result.

1 Introduction

Swarms of starlings, schools of fish, and herds of animals show a remarkable property: complex collective behavior emerges from simple individual decisions. Collective motion is studied across physics, biology, computer science, and robotics [1–4]. The foundational mathematical description is the Vicsek model [1]: point-like agents move at constant speed and align their heading with the average heading of their neighbors, disturbed by noise. Many later models, including the Boids model [5], build on this idea.

A key modeling decision is hidden in the word “neighbors”. *Metric* models let an agent interact with everyone inside a fixed radius r. *Topological* models let it interact with a fixed number k of nearest agents, regardless of distance. Observations of real bird flocks support topological interactions [6], and topological models show richer phase behavior [7]. However, in the regimes studied in this thesis, purely topological selection destabilizes the Vicsek dynamics: the swarm fragments into many small, short-ranged packets instead of forming large coherent structures.

This manuscript summarizes the two contributions of the underlying bachelor thesis:

1. A **stochastic metric-topological neighbor rule**, introduced in this thesis, that keeps the fixed neighbor count of topological models while recovering the stability of the metric Vicsek model. Its agreement with the Vicsek model is evaluated quantitatively.

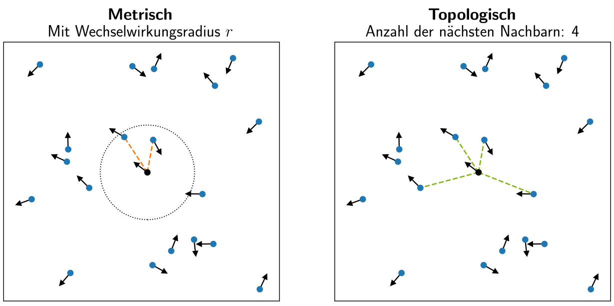

Figure 1: Metric versus topological neighbor selection. Left: a metric agent (black) interacts with all agents inside its radius r (dotted circle, orange links). Right: a topological agent interacts with its $k = 4$ nearest agents (green links), however far away they are. Figure from the thesis; panel titles are in German (“Metrisch” means metric, “Topologisch” means topological).

2. An exploratory **multi-agent reinforcement learning (MARL) extension** in which agents were meant to learn alignment behavior from a global objective instead of a fixed local rule. The pipeline was implemented and ran, but training was not successful. It is included as an honest negative result.

2 Background: the Vicsek model

The Vicsek model [1] describes N agents in a square box of side length L with periodic boundaries. All agents move at the same constant speed v_0. The only degree of freedom of agent i is its heading θ_i. Positions advance with a simple Euler step,

$$\tilde{\vec{x}}_i(\tilde{t}+1) = \tilde{\vec{x}}_i(\tilde{t}) + \tilde{\vec{v}}_i(\tilde{t})\,\Delta\tilde{t}, \tag{1}$$

where all quantities are made dimensionless with the interaction radius r and the speed v_0. The new heading is the average heading of all neighbors within the radius r (including the agent itself) plus a noise term,

$$\theta_i(\tilde{t}+1) = \langle\theta(\tilde{t})\rangle_r + \Delta\theta, \qquad \Delta\theta \sim \mathcal{U}\left[-\tfrac{\eta}{2}, \tfrac{\eta}{2}\right], \tag{2}$$

with the circular average

$$\langle\theta(\tilde{t})\rangle_r = \arctan\left[\frac{\langle\sin\theta(\tilde{t})\rangle_r}{\langle\cos\theta(\tilde{t})\rangle_r}\right]. \tag{3}$$

The noise strength η controls the macroscopic state. The degree of global alignment is measured by the order parameter

$$v_a = \frac{1}{N v_0}\left|\sum_{i=1}^{N}\vec{v}_i\right| \in [0,1], \tag{4}$$

which is 1 for a perfectly aligned swarm and close to 0 for a disordered one. Following the original work, all simulations use $v_0 = 0.03$ (in units of r per step) and are evaluated through v_a as a function of η, N, and the density $\rho = N/L^2$.

Figure 1 illustrates the two established neighbor definitions. The topological variant replaces the radius criterion in Eq. (3) with the k nearest agents.

2.1 Why purely topological selection fails here

Fixing the number of interaction partners is attractive: it makes the input size of each agent constant, which matters both for biological plausibility and for machine learning, where network inputs have a fixed dimension. In practice, however, the purely topological Vicsek variant behaves poorly in the investigated regimes. In regions of high local density the k nearest neighbors are all very close, so interactions become effectively short-ranged. Small packets of mutually aligned agents form, decouple from the rest, and the global order parameter collapses already at very small noise (top row of Figure 2; see also Figure 3).

A naive repair, taking the k nearest neighbors and discarding all of them beyond the radius r, makes things worse: it removes exactly the long-ranged part of the interaction that was still present.

3 The stochastic metric-topological rule

The model introduced in this thesis keeps both structural elements: the metric radius r and the fixed neighbor count k. The rule is:

1. Collect all agents within the metric radius r (the Vicsek candidate set).
2. If this set holds more than k agents, draw k of them uniformly at random, without replacement. Otherwise keep all.
3. Apply the Vicsek average, Eq. (3), to the sampled set (plus the agent itself).

The draw is repeated independently for every agent and every time step, so the interaction graph is resampled continuously.

Intuition. Figure 4 shows the idea that led to the rule. Seen from one agent, the neighborhood is a radial histogram of headings. If the agent can only process k inputs, a sensible compression is to divide the histogram into k regions of equal agent count (k-quantiles) and average within each region. Computing quantiles explicitly every step is expensive. Random sampling achieves the same effect statistically: over many steps, uniform draws hit each equal-count region equally often.

Monte Carlo interpretation. The quantities that enter the Vicsek average are the sample means of $\sin\theta$ and $\cos\theta$ over the selected neighbors. Under uniform sampling without replacement, these sample means are unbiased estimators of the means over the full metric neighborhood. Each update is therefore a Monte Carlo estimate of the exact Vicsek update, with k in the role of the sample size. This view makes a clear prediction: the model should converge to the metric Vicsek model as k grows. Section 5 confirms this empirically. No variance or error control was implemented; the estimate is simply plugged into the dynamics at small fixed k.

4 Simulation and validation

The simulation core is written in C++ [8] and exposed to Python [9] through pybind11 [10]. C++ handles the performance-critical parts, Python handles orchestration, analysis, and plotting with Matplotlib [11]. The core solves four recurring tasks:

- **Cell decomposition.** The box is divided into square cells of edge length $2r$ and agents are assigned to cells. The neighbor search then only inspects a small cell neighborhood instead of all $\mathcal{O}(N^2)$ pairs.
- **Neighbor determination.** All model variants share one neighbor routine; the metric, topological, and metric-topological rules differ only in the final selection step. This step dominates the runtime and is the only part that is parallelized with OpenMP.
- **Periodic boundaries.** Distances and cell lookups are corrected for wrap-around, which has to be respected at several layers of the code.

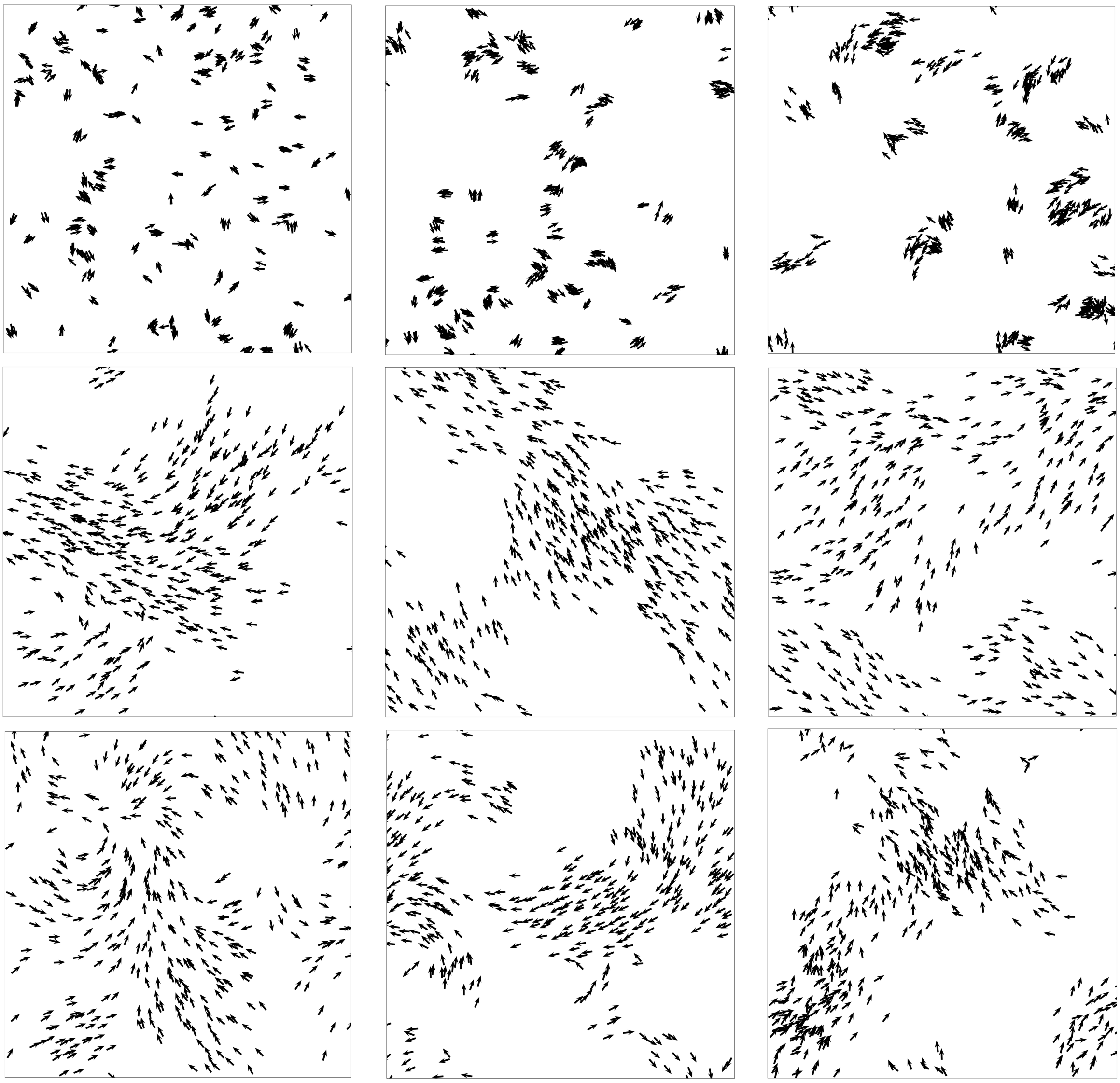

Figure 2: Snapshots of the three models after few simulation steps, with $N = 400$ and $\rho = 4$. Columns from left to right: $\eta = 0.4$ ($k = 1$), $\eta = 0.6$ ($k = 2$), $\eta = 1.0$ ($k = 4$). Top row: purely topological model. The swarm fragments into many small aligned packets. Middle row: the stochastic metric-topological model introduced in this thesis. Although only k neighbors are used per step, large stream-like structures form. Bottom row: metric Vicsek reference. The middle row resembles the bottom row far more than the top row does.

- **Synchronous updates.** All agents are updated from the same previous state, as in the original model.

Large runs are written as `.xyz` trajectories and rendered with OVITO [12], a visualization tool from solid state physics that handles up to 10^5 agents in real time. In addition, an interactive Matplotlib front end with live sliders for η, r, and k, an optional cell grid overlay, and per-neighbor distance lines was built for visual debugging. This visual inspection layer proved essential for catching boundary and neighbor selection errors that unit checks missed.

Before any comparison between models, the metric baseline itself was validated against the original publication. Figure 5 reproduces the classic order parameter versus noise measurement of Vicsek et al. [1]. The curves agree qualitatively over the full noise range; quantitative deviations at high noise ($\eta \gtrsim 3$) remain and several candidate error sources (neighbor search, boundary handling, random number generators, statistical protocol) were checked and excluded in the thesis. Stability of the measured values was checked by varying simulation length and initial conditions, including fully ordered starts; results converged to the same values.

5 Results

Stability. The middle row of Figure 2 shows the qualitative result. Although each agent uses only k neighbors per step, the fragmentation of the purely topological model disappears. The swarm forms large

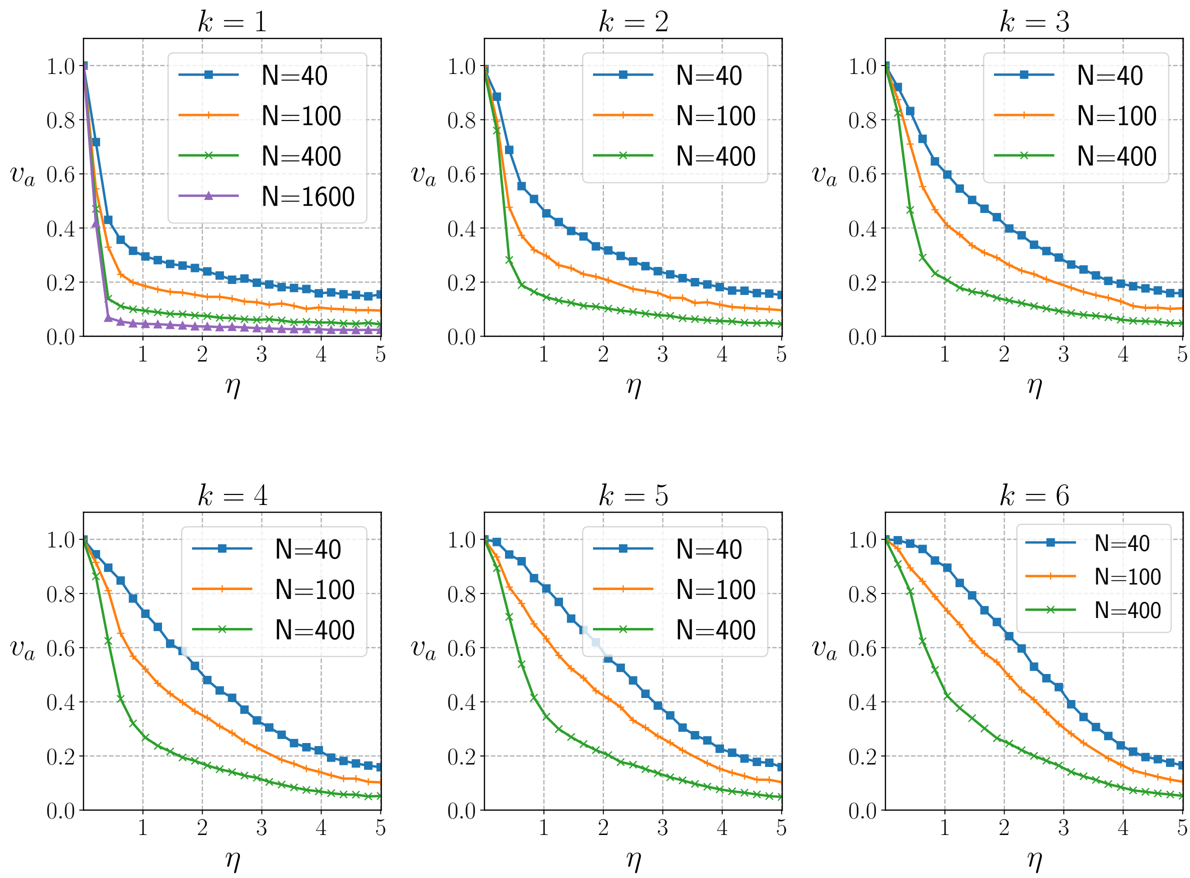

Figure 3: Order parameter v_a versus noise η for the purely topological model at constant density $\rho = 4$, for $k = 1$ to 6 neighbors and several system sizes. For small k the order parameter collapses already at very small noise values, and larger systems are affected more strongly. This instability motivates the metric-topological rule.

stream-like structures that resemble the metric Vicsek reference. One visible difference remains: sharp vortex-like turns of the metric model are smoothed out for small k, because an agent cannot process all incoming directions in a single step.

Convergence to the Vicsek model. For $k \geq N$ the rule keeps every candidate and reduces exactly to the metric Vicsek model, so convergence in k is expected. The Monte Carlo interpretation predicts that it should be fast. Figure 6 shows $v_a(\eta)$ for $k =$ 1 to 6 with the squared deviation from the Vicsek reference drawn as a tube around each curve. Figure 7 condenses this into a single number per configuration: the mean squared deviation falls by more than an order of magnitude from $k = 1$ to $k = 6$, approximately as a power law in k, and for $k = 6$ the two models are practically indistinguishable under this observable. Larger systems converge more slowly at equal density.

These statements are limited to the evaluated observable (v_a as a function of η), the evaluated densities, and system sizes up to $N = 1600$ for the quantitative comparison. No claim of general equivalence is made.

Density-based order parameter. The alignment parameter v_a says nothing about how compact a swarm is: a system of many small, internally aligned packets and one large coherent flock can score identically. To close this gap, the thesis additionally introduced a distance-weighted order parameter,

$$\rho_a \propto \sum_{i<j}^{N} \tilde{\vec{v}}_i \cdot \tilde{\vec{v}}_j \left(\left| \tilde{\vec{x}}_i - \tilde{\vec{x}}_j \right|^2 + d^2 \right)^{-\alpha/2}, \tag{5}$$

where the smoothing scale d caps the contribution of very close pairs and α controls how strongly distance is weighted. Pairs that are aligned and close contribute most, so ρ_a rewards compact coherent swarms. It was implemented and measured for the metric-topological model, but only studied phenomenologically. Such parameters are also natural candidates for reward signals in the learning experiments of the next section, because they encode a global goal in a single scalar.

6 Reinforcement learning extension

The second goal of the thesis was a change of perspective: instead of prescribing a local interaction rule, define a global objective and let the agents learn the rule. The order parameter Eq. (4) is a natural reward

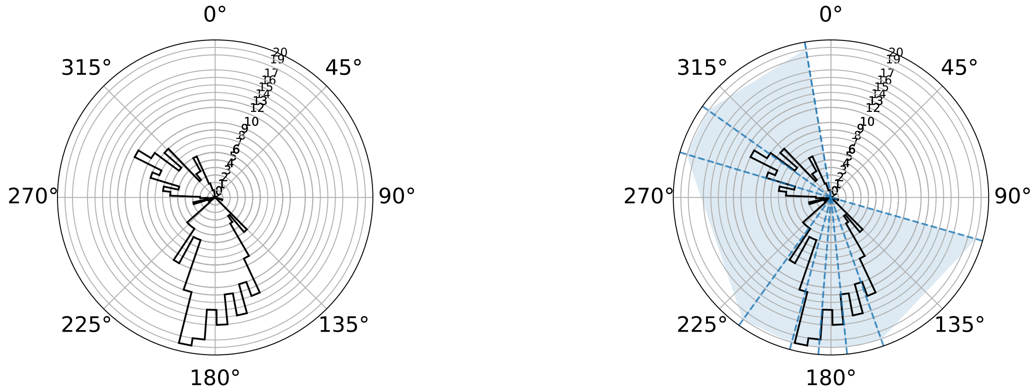

Figure 4: Conceptual motivation, shown for synthetic data. Left: a radial histogram of the headings an agent sees inside its interaction radius. Two larger groups with different orientations are visible. Right: the same histogram divided into k-quantiles (here $k = 8$, dashed lines), regions that contain equal numbers of agents. Averaging one representative per region compresses the full neighborhood into k inputs without discarding any direction of the sky. The random sampling rule realizes this averaging over time.

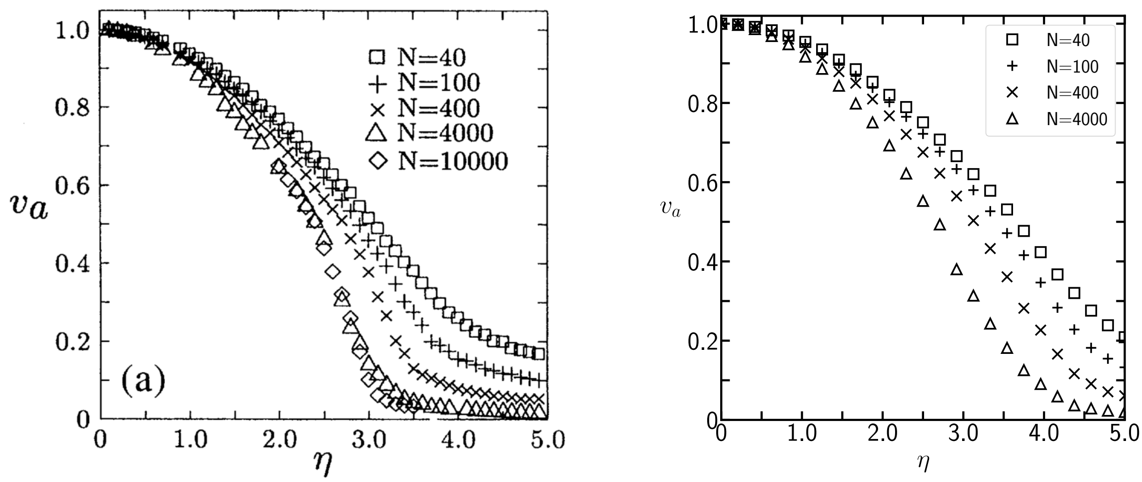

Figure 5: Validation of the simulation core. Left: the original measurement from Vicsek et al. [1], order parameter v_a versus noise η at constant density. Right: the same experiment reproduced with the simulation written for this thesis. The qualitative course agrees; deviations appear for large noise ($\eta \gtrsim 3$) and are discussed in the thesis.

signal, since the Vicsek rule itself drives v_a upward. The metric-topological model was designed with this in mind, because its fixed k gives every agent an observation vector of constant size.

Setup. Figure 8 shows the conceptual architecture. The C++ simulation was wrapped as a learning environment through pybind11: a dedicated simulation class hands each agent the headings of its k sampled neighbors as the observation, accepts a new heading in $[0, 2\pi]$ as the continuous action, and reports the change of the global order parameter as the reward. On this environment an actor-critic pipeline [13–15] was trained, with the minimal actor of Figure 9 and a standard critic. A second attempt used a multi-agent environment with one agent per particle and a shared policy in RLlib [16].

Outcome. The pipeline ran end to end: environment, replay buffer, actor, critic, and training loop all worked together, and training proceeded. The results, however, were not interpretable. The main identified problem was the representation of the angle: a heading is a periodic quantity, and feeding it to the networks as a plain scalar in $[0, 2\pi]$ creates a discontinuity at the wrap-around that the simple networks did not overcome in the available time. The RLlib attempt failed earlier, at training launch. No successful or partially successful policy was obtained, and no conclusion about the learnability of the Vicsek rule can be drawn from these experiments. What the thesis does establish is that the simulation is fully embeddable in standard MARL tooling, and it formulates the natural next experiment: testing whether a single-layer perceptron with a periodic angle encoding (for example $\sin\theta$, $\cos\theta$) can learn the averaging rule.

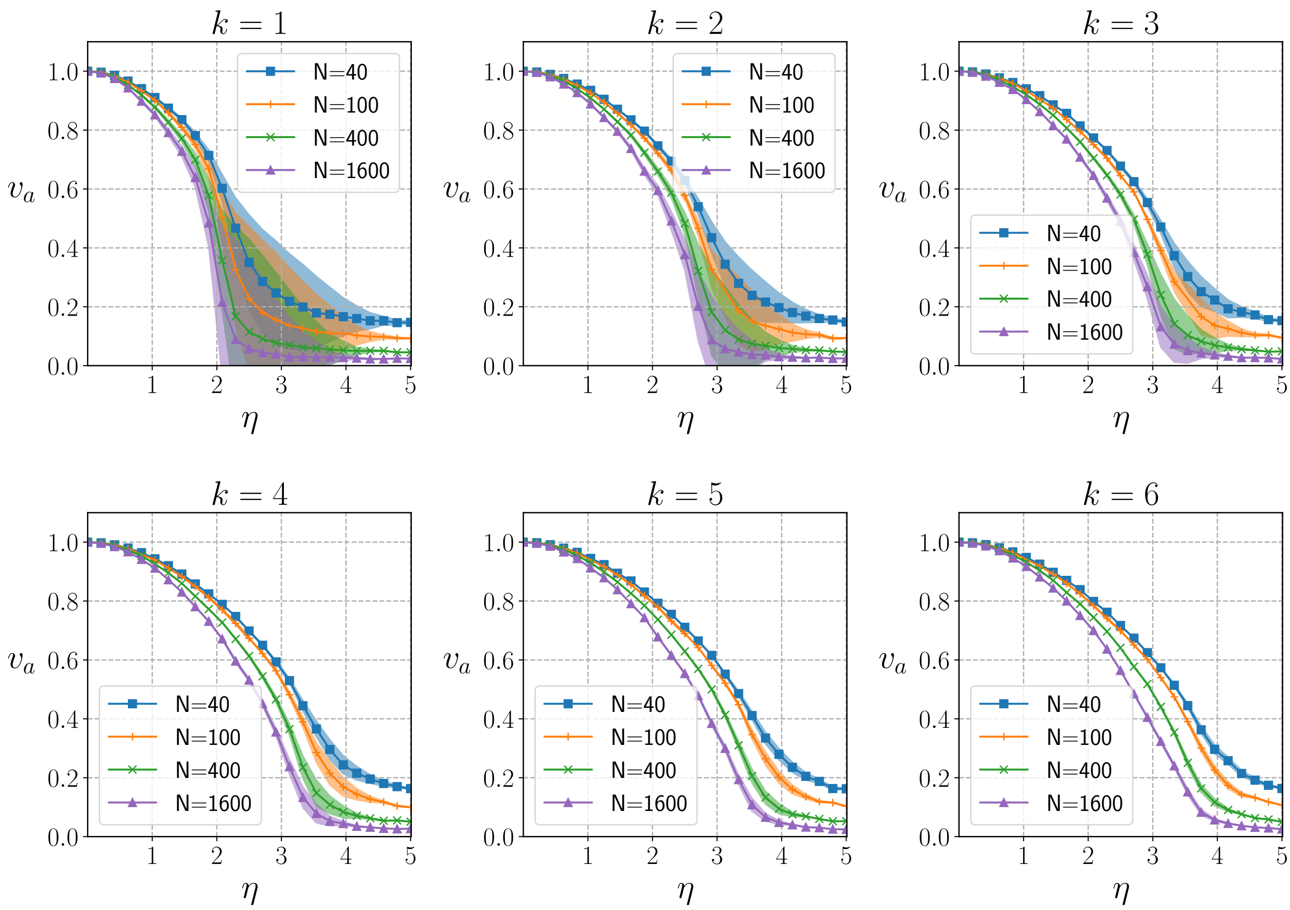

Figure 6: Convergence of the stochastic metric-topological model toward the metric Vicsek model at constant density $\rho = 4$. Each panel shows $v_a(\eta)$ for one value of k and several system sizes; the shaded tube around each curve is the squared deviation from the Vicsek reference. The tubes shrink quickly with growing k; for $k = 6$ the deviations are barely visible.

7 Limitations and outlook

The scope of the positive result is deliberately narrow. Agreement with the Vicsek model was shown for the alignment order parameter v_a under the evaluated noise values, densities, and system sizes. Other observables, such as correlation functions or the density-based order parameter, were only touched on. The statistical protocol used running averages without advanced error analysis, and the high-noise deviation from the original Vicsek data remains unexplained. The reinforcement learning part is a documented negative result and should be read as such.

Natural continuations are: a periodic encoding of the heading for the learning experiments; a variance analysis of the sampling rule to put the Monte Carlo view on quantitative footing; and a study of the model in regimes where metric and topological models genuinely disagree, to see which behavior the mixed rule follows.

The lasting value of the project is the combination of an original, validated modeling idea with an early, honest attempt to connect physical simulation and multi-agent learning.

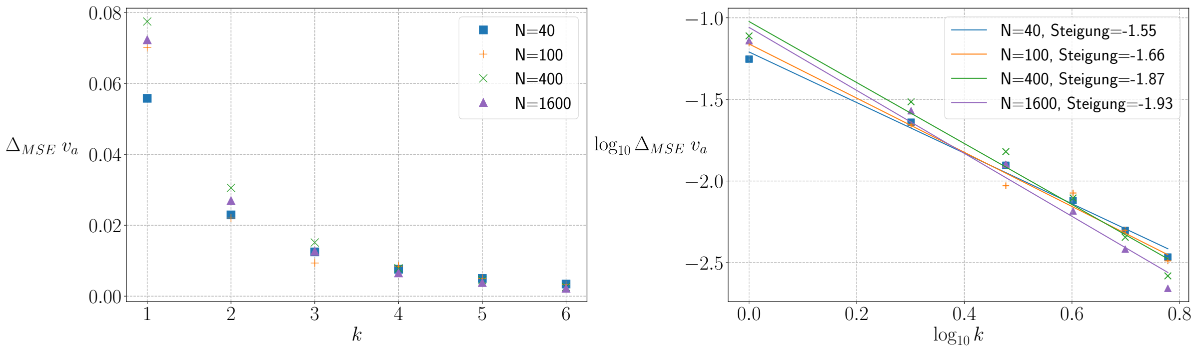

Figure 7: Quantitative convergence in the sample size k. Left: mean squared deviation of v_a between the metric-topological model and the self-generated Vicsek reference, for each system size and $k = 1$ to 6. Right: log-log representation with linear fits (the German legend word "Steigung" means slope). The deviation follows an approximate power law in k with fitted slopes between -1.55 and -1.93; larger systems converge more slowly at equal density.

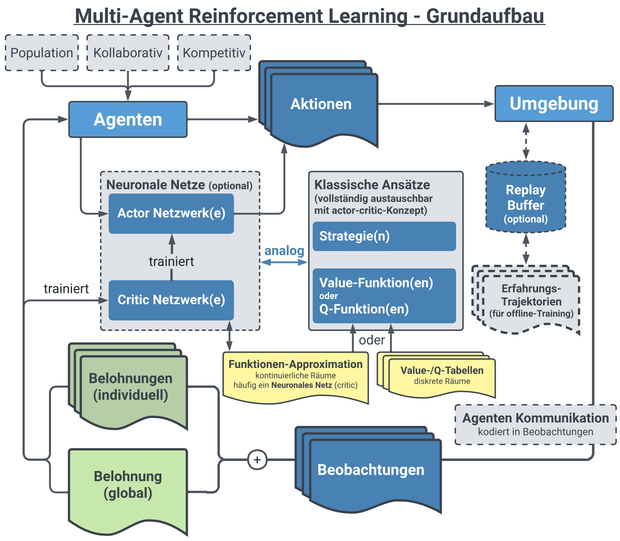

Figure 8: Conceptual MARL setup drawn for the thesis: agents act in a shared environment, observations and rewards flow back, and an actor network selects actions while a critic network estimates their value. Labels are in German ("Agenten" agents, "Aktionen" actions, "Umgebung" environment, "Belohnungen" rewards, "Beobachtungen" observations).

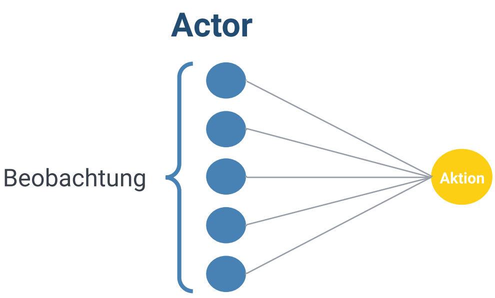

Figure 9: The actor network used in the experiments ("Beobachtung" means observation, "Aktion" means action). It was kept deliberately minimal (a single dense layer) because the target behavior, the Vicsek averaging rule, is itself a simple function of the observed neighbor headings.

References

[1] T. Vicsek et al. "Novel Type of Phase Transition in a System of Self-Driven Particles". In: *Physical Review Letters* 75 (1995), pp. 1226–1229. DOI: 10.1103/PhysRevLett.75.1226.

[2] T. Vicsek and A. Zafeiris. "Collective motion". In: *Physics Reports* 517 (2012), pp. 71–140. DOI: 10.1016/j.physrep.2012.03.004.

[3] S.-J. Chung et al. "A Survey on Aerial Swarm Robotics". In: *IEEE Transactions on Robotics* 34 (2018), pp. 837–855. DOI: 10.1109/TRO.2018.2857475.

[4] D. St-Onge et al. "Collective expression: how robotic swarms convey information with group motion". In: *Paladyn, Journal of Behavioral Robotics* 10 (2019), pp. 418–435. DOI: doi:10.1515/pjbr-2019-0033.

[5] C. W. Reynolds. "Flocks, herds and schools: A distributed behavioral model". In: *ACM SIGGRAPH Computer Graphics*. Vol. 21. 4. ACM. 1987, pp. 25–34. DOI: 10.1145/37401.37406.

[6] M. Ballerini et al. "Interaction ruling animal collective behavior depends on topological rather than metric distance: Evidence from a field study". In: *Proceedings of the National Academy of Sciences* 105 (2008), pp. 1232–1237. DOI: 10.1073/pnas.0711437105.

[7] P. Rahmani, F. Peruani, and P. Romanczuk. "Topological flocking models in spatially heterogeneous environments". In: *Communications Physics* 4 (2021), p. 206. DOI: 10.1038/s42005-021-00708-y.

[8] I. J. .-. T. C. S. Committee. *ISO International Standard ISO/IEC 14882:2014(E) – Programming Language C++*. 2014. URL: https://www.iso.org/standard/64029.html.

[9] P. S. Foundation. *Python 3.10.0 Documentation*. 2021. URL: https://docs.python.org/3.10/.

[10] W. Jakob et al. *pybind11 – Seamless operability between C++11 and Python*. Available at https://github.com/pybind/pybind11. 2016.

[11] J. D. Hunter. "Matplotlib: A 2D graphics environment". In: *Computing in Science & Engineering* 9 (2007), pp. 90–95. DOI: 10.1109/MCSE.2007.55.

[12] A. Stukowski. "Visualization and analysis of atomistic simulation data with OVITO - the Open Visualization Tool". In: *Modelling and Simulation in Materials Science and Engineering* 18 (2010). Available at http://ovito.org/, p. 015012.

[13] T. P. Lillicrap et al. *Continuous control with deep reinforcement learning*. 2019. arXiv: 1509.02971 [cs.LG].

[14] *TF-Agents: Reliable and Easy-to-use TensorFlow library for building Reinforcement Learning models*. URL: https://github.com/tensorflow/agents.

[15] Martín Abadi et al. *TensorFlow: Large-Scale Machine Learning on Heterogeneous Systems*. Software available from tensorflow.org. 2015. URL: https://www.tensorflow.org/.

[16] *RLlib: An Open-Source Library for Reinforcement Learning*. URL: https://github.com/ray-project/ray.